UDC [622.02:539.2/.8]:622.831.325 DOI: https://doi.org/10.15407/geotm2024.170.055

MATHEMATICAL MODEL OF THE FAILURE OF TALL PRISMATIC ROCK SAMPLES WITH A HIGH INTERNAL FRICTION ANGLE

Vasyliev L., Vasyliev D., Krasovskyi I., Rizo Z., Kress D.

M.S. Poliakov Institute of Geotechnical Mechanics of the National Academy of Sciences of Ukraine

Abstract. The mechanical properties of rocks are among the most critical factors determining their resistance to failure, particularly significant in the context of the mining industry and underground operations. Traditionally, such tests have been regulated by state standards (GOSTs) involving the crushing of samples with regular geometries, such as cubes, prisms, and cylinders. The primary objective of these standards is to determine the compressive strength limit, a key indicator for assessing material stability under load.

Tests are conducted on specimens with heights slightly exceeding their cross-sectional dimensions, enabling a more accurate simulation of rock behavior under real geological conditions. A major parameter for analyzing the stress-strain state of rocks is the strength limit and residual strength, evaluated through "stress-strain" diagrams obtained during sample failure.

Such characteristics are typically determined using specialized presses available in major research centers like the Institute of Geotechnical Mechanics of the National Academy of Sciences of Ukraine and the Kryvyi Rih National Technical University. However, this equipment demands skilled personnel, regular maintenance, and is often distant from mining sites, creating challenges in obtaining timely information about rock strength - an essential factor for mining safety.

This article introduces a new analytical method for calculating the strength and residual strength of rocks, based on more accessible and straightforward tests. This method facilitates the determination of four key parameters: shear strength limit, coefficients of internal and contact friction, and the material's elastic modulus.

The proposed approach not only simplifies the evaluation of strength characteristics but also provides a more accurate description of failure processes in taller samples, which is crucial for engineering calculations and the design of mining structures. Research findings indicate that increasing the sample height significantly reduces its strength; for instance, doubling the height can decrease the ultimate strength by up to 30%.

Consequently, the proposed analytical method enhances the ability to obtain rock strength data directly in the field, enabling swift stability assessments and reducing the risk of accidents. This contributes to improving efficiency and safety in mining operations through more precise predictions of rock behavior under load. The method is valuable for both research and practical applications, offering engineers and designers a tool for more detailed analysis of rock strength characteristics.

Keywords: rock, strength limit, failure, crack, stress-strain diagram.

1. Introduction

The mechanical properties of rocks play a key role in ensuring the stability of structures and the efficiency of mining operations. Testing samples to determine the material's strength limit is regulated by national standards in many countries. These tests often rely on compressing samples of regular geometric shapes, such as cubes, prisms, or cylinders. European standards, for example, recommend a height-to-diameter or height-to-length ratio of two for the samples to minimize the impact of contact friction.

Given Ukraine's integration into the European Union, there is a growing need to adapt existing standards to European requirements. However, the effect of sample geometric parameters on reducing contact friction and, consequently, on the accuracy of strength limit determination remains underexplored.

Existing literature offers various approaches to modeling rock failure processes. For instance, studies [1–4] analyze the failure mechanisms of tall prismatic samples considering the internal friction angle. Works [5–8] explore modern methods for modeling the stress-strain state of rocks, including the use of discrete fracture net-

work models. Furthermore, classic studies [9–10] provide a theoretical foundation for understanding the mechanical properties of rocks.

The objective of this study is to investigate the influence of sample geometry on the strength limit and to develop an analytical method that accounts for these parameters. A comparative analysis of data is also conducted for samples of regular geometry and tall samples using methods proposed in the literature [1–10].

2. Methods

The authors of the article, based on the theory of slip lines in solid body deformation mechanics, have developed several analytical methods for calculating strength limits and the parameters of "stress-strain" diagrams for prismatic samples with a high degree of convergence with experimental data. These methods are applied to some of the known failure modes under uniaxial compression according to L.I. Baron – truncated wedge, longitudinal, wedge, and diagonal forms – using an exponential distribution of contact normal stresses according to E.P. Unksov. One of the conditions for the formation of rock sample failure modes is the intersection of one of the slip lines with the vertical symmetry line of the sample, resulting in a wedge-shaped form. It is clear that as the height of the sample increases, the probability of transforming truncated-wedge and longitudinal forms into wedge or diagonal forms increases. As experts understand, the strength limit of rocks without contact friction is precise. However, when testing samples under compression, there is no way to eliminate contact friction between the sample and the plates. Experimenters have noticed that as the sample height increases, its strength decreases. However, it is unclear how much this decrease brings the experimenter closer to the true strength. Therefore, we have set the goal of developing an analytical method for calculating the strength limits of tall samples and comparing them with methods for calculating samples of regular geometry, i.e., when their height equals the length (or width).

To describe the rock failure process, the Coulomb criterion for maximum effective shear stresses on slip lines and on slip surfaces (SS), in our opinion, is more appropriate. The Coulomb criterion [4] for cohesive media is based on the assumption that the rock's resistance to shear τ on a given slip surface is equal to the sum of the resistance to pure shear (shear strength limit) and a term proportional to the normal stress σ on that surface (compression is considered positive). Upon failure of the sample on the SS, a crack forms. As the crack develops, part of the material is relieved of load. Given the plane strain model, the bearing portion of the material at any moment can be determined from the coordinates of the tip of one or two cracks, which corresponds to the original area of the sample minus the part that has been relieved of load as the crack develops along the SS. The relieved portion of the sample is determined by the abscissa values of the crack tip as $x = yctg\alpha$, where y – ordinate of the axis OY, α – the angle of inclination of the left slip surface (SS) at the crack tip relative to the x-axis (abscissa axis).

As the conceptual basis for developing the method of calculating the strength of tall samples, we use the method of calculating basing on practical researches prismatic samples of regular geometry [1, 4]. In Figure 1, we depict the sample. A verti-

cal load acts on the sample, along with contact shear stresses arising from contact friction, which are directed inward, opposing transverse deformation. The coordinate axes are placed in the top-left corner of the sample. On the upper surface of the left longitudinal half of the sample, the contact shear τ_c stresses are positive, while on the lower surface, they are negative. On the right half, the signs of the stresses are opposite. It is important to note that due to the vertical load, the sample acquires a convex shape. Therefore, the rule of parity for shear stresses is applicable at the corners of the sample. The derivation of the formulas for determining the parameters of the sample's failure is presented in [3–8].

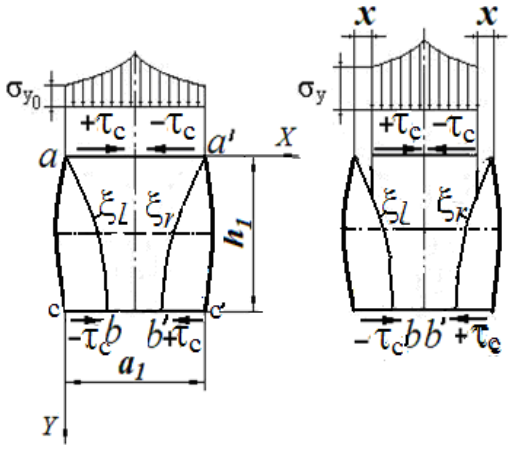

Figure 1 – Diagram of the formation of an exponential profile of contact normal stresses and the development of two cracks along SL (slip line) ξ under the distribution according to formula (2)

The angle of inclination of the slip line ξ relative to the horizontal is determined by the formula:

$$\alpha_\xi = \frac{\pi}{4} + \frac{\rho}{2} + \beta_\xi, \tag{1}$$

where ρ – angle of internal friction, rad; β_ξ – angle of rotation of the left slip line from contact friction, rad.

The well-known formulas for calculating the normal compressive stress σ_y along the length of the sample and the specific contact pressure according to E. N. Unksov [4] were used.

$$\sigma_{y_i} = \sigma_{y_0}\, exp\left(\frac{2 f_c \cdot x}{h_1}\right); \tag{2}$$

$$p = \sigma_{y_0} \frac{h_1}{f_c \cdot a_1}\left(exp\left(\frac{f_c \cdot a_1}{h_1}\right) - 1\right), \tag{3}$$

where σ_{y_0} – normal tension at angular point, Pa; f_c – contact friction coefficient; a_1 and h_1 – specimen length and height, m.

Vertical normal tension on left SL ξ_1 is determined by the formula

$$\sigma_{y_\xi} = \frac{1}{\mu}\left(\frac{k_n\left(1+sin\,\rho\sqrt{1-b_\xi^2}\right)\cdot exp\left(2\mu\left(\beta_\xi+\beta_b\right)\right)}{1-sin\,\rho\sqrt{1-b_b^2}} - k_b \right), \tag{4}$$

where k_n – material shear resistance, Pa; μ= tgρ – internal friction coefficient;

$$k_b = \frac{\left(k_n+\mu\sigma_y\right)\left(1-sin\,\rho\sqrt{1-b_\xi^2}\right)}{\left(1+sin\,\rho\sqrt{1-b_b^2}\right)exp\left(4\mu\beta_c\right)} \tag{5}$$

k_b – shear resistance of a material by SL ξ_1 on the side of the lower contact plane, Pa.

Taking into account the exponential regularity of normal stresses according to E.P. Unksov [4], where b_ξ and b_b:

$$b_\xi = \frac{f_c\left(1-\frac{2y}{h_1}\right)\cdot\sigma_{y_\xi}\cdot exp\left(\frac{2f_c\cdot x_\xi}{h_1}\right)}{k_n+\mu\sigma_{y_\xi}\cdot exp\left(\frac{2f_c\cdot x_\xi}{h_1}\right)}; \tag{6}$$

$$b_b = -\frac{f_c\cdot\sigma_{y_\xi}\cdot exp\left(\frac{2f_c\cdot x_b}{h_1}\right)}{k_b+\mu\sigma_{y_\xi}\cdot exp\left(\frac{2f_c\cdot x_b}{h_1}\right)}, \tag{7}$$

where x_ξ – current value of the crack apex abscissa by SL ξ, m; x_b– abscissa of the intersection point of SL ξ with the lower surface of the specimens, m.

But it should be emphasized here that since the edge of the sample is out of load, the stress $\sigma_{y\xi}$ at the top of the crack for the left SL ξ plays the role of tension σ_{y0} – vertical normal stress at the angular point. Therefore, in formulas (5–7) it is necessary to use $\sigma_{y\xi} = \sigma_{y0}$. Note that the stress values $\sigma_{y\xi}$ with increasing ordinate y_ξ increase. Using b_ξ and b_b to calculate normal stress $\sigma_{y\xi}$ important parameters are determined β_ξ rad and β_b, rad:

$$\beta_\xi = \frac{1}{2} arctg \frac{b_\xi \cos\rho}{\sin\rho - \sqrt{1 - b_\xi^2}}; \quad (8)$$

$$\beta_b = \frac{1}{2} arctg \frac{b_b \cos\rho}{\sin\rho - \sqrt{1 - b_b^2}}. \quad (9)$$

From here, we provide a description of the left SL ξ. The rotation angle β_b on the lower (supporting) contact surface will have a negative sign, and for each condition ξ, it will be constant. On the lower surface, the equality k_b=k_n holds when the crack reaches the lower surface; in the rest of the sample area on the left SL ξ, the inequality k_b<k_n is satisfied. After this, it becomes possible to determine the value of the normal stress $\sigma_{y0} = \sigma_{y\xi}$ on SL ξ, using a system of equations.

With the development of two symmetrical cracks along SL ξ (Fig. 1), the formula for the specific force will take the form:

$$p = \frac{2\int_0^t \sigma_{y_\xi} \exp\left(\frac{2f_c \cdot t}{h_1}\right) dt}{\left(a_1 - 2x_\xi\right)} = \sigma_{y_\xi} \frac{h_1}{f_c\left(a_1 - 2x_\xi\right)}\left(\exp\left(\frac{f_c}{h_1} \cdot \left(a_1 - 2x_\xi\right)\right) - 1\right), \quad (10)$$

where $t = \frac{a_1}{2} - x$; σ_{y_ξ} – normal stress at the crack apex; x_ξ – current value of the crack apex abscissa by ξ.

Using the presented formulas, we obtain a set of theoretical curves in the form of "normal stress – longitudinal strain" diagrams, which can be compared for reliability with experimental data [4] (Fig. 2).

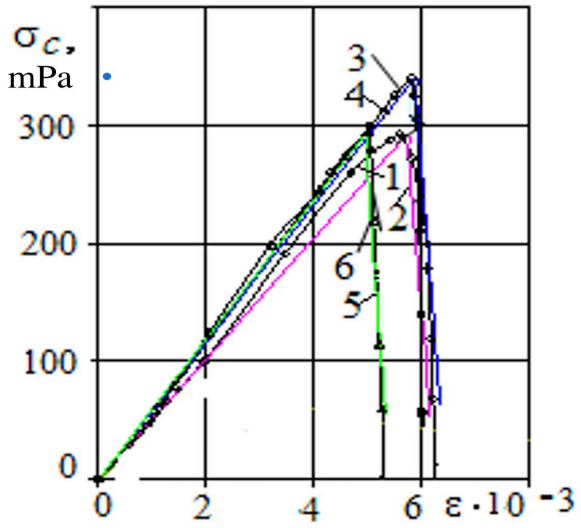

Figure 2 – Stress-longitudinal strain diagrams
with a truncated wedge form of destruction of high specimens

The authors of [4] do not provide the necessary physical and mechanical characteristics, such as the material's shear resistance and the coefficients of external and internal friction. These can be approximately determined based on the appearance of the ultimate curves, allowing for a very close match between the calculated and experimental strength limits. For instance, experimental diagram 1 is described by calculated diagram 2 when: $k_n = 60$ MPa, $\mu = 1.0$, $f_c = 0.02$, $E = 5.1 \cdot 10^4$ MPa, experimental diagram 3 – calculation diagram 4 at $k_n = 69$ MPa, $\mu=1.0$, $f_c = 0.02$, $E=5.8 \cdot 10^3$ MPa; experimental diagram 5 – calculation diagram 6 at $k_n = 59$ MPa, $\mu = 1$, $f_c = 0.02$, $E = 5.9 \cdot 10^3$ MPa.

The comparison of calculated diagrams with experimental diagrams obtained under uniaxial compression convincingly demonstrates the high effectiveness of the proposed method for calculating the strength limit and constructing ultimate failure curves for rocks.

In general, it should be noted that the highest agreement with experimental data is observed for the exponential distribution of shear stresses when the stabilization of the contact friction coefficient fc is within the range of 0.2 to 0.35. From the analysis, an important conclusion emerges: the exponential distribution of contact shear stresses ensures satisfactory reliability of the calculated strength limit results when compared with experimental data for fc values within the range of 0.2 to 0.35.

When f_c exceeds 0.35–0.4 and ρ exceeds 40°, a longitudinal failure shape is formed instead of a truncated-wedge shape. This longitudinal failure shape will be described in a subsequent article. The criterion for the formation of the truncated-wedge shape is the alignment of SL ξ_l and ξ_r with the corresponding half of the sample.

Next, let us consider the calculation of tall samples. For example, we take a prismatic sample with the following rock material properties: k_n=10 MPa, μ=1, f_c=0.25, E=5.9·10^4 MPa.

Using these values in the calculation, we obtain a truncated-wedge failure shape for the sample, as shown in Fig. 1. Let us take a tall sample with a height h=1.15·a_1, at which point SL ξ_l reaches the vertical line of symmetry (Fig. 3), resulting in no residual strength.

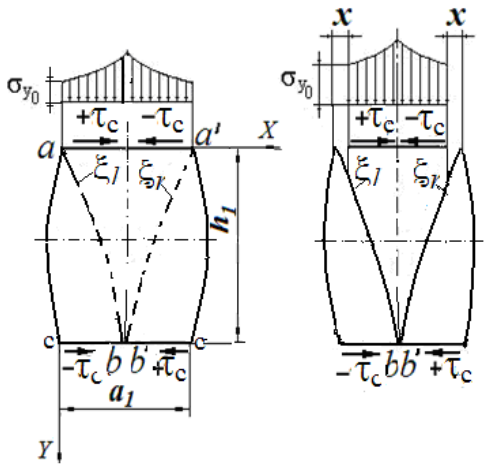

Figure 3 – Stress state diagram of a tall specimen in the absence of residual strength

The comparison of calculated diagrams with experimental diagrams obtained under uniaxial compression convincingly demonstrates the high effectiveness of the proposed method for calculating the strength limit and constructing ultimate failure curves for rocks.

In general, it should be noted that the highest agreement with experimental data is observed for the exponential distribution of shear stresses when the stabilization of the contact friction coefficient f_c is within the range of 0.2 to 0.35. From the analysis, an important conclusion emerges: the exponential distribution of contact shear stresses ensures satisfactory reliability of the calculated strength limit results when compared with experimental data for f_c values within the range of 0.2 to 0.35.

When f_c exceeds 0.35–0.4 and ρ exceeds 40°, a longitudinal failure shape is formed instead of a truncated-wedge shape. This longitudinal failure shape will be described in a subsequent article. The criterion for the formation of the truncated-wedge shape is the alignment of SL ξ_l and ξ_r with the corresponding half of the sample.

Next, let us consider the calculation of tall samples. For example, we take a prismatic sample with the following rock material properties: k_n = 10 MPa, μ = 1.0, f_c = 0.25, $E = 5.9 \cdot 10^4$ MPa.

Using these values in the calculation, we obtain a truncated-wedge failure shape for the sample, as shown in Fig. 1. Let us take a tall sample with a height h = 1, at which point SL ξ_l reaches the vertical line of symmetry (Fig. 4), resulting in no residual strength

$$\alpha_\eta = \frac{7}{4}\pi - \frac{\rho}{2} - \beta_r . \qquad (11)$$

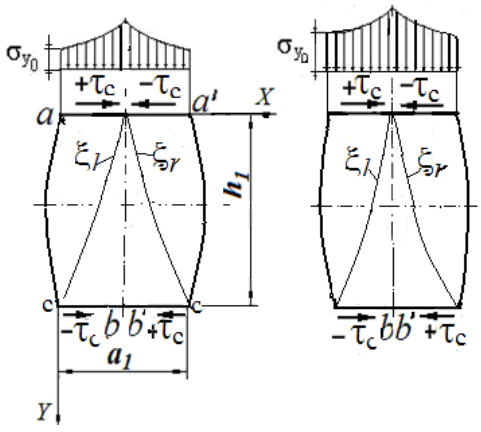

Figure 4 – High specimen pre-fracture scheme h_1=1.15·a_1

Now, let's take a sample with a height, for example, equal to $h_1 = 1.5 \cdot a_1$ (Fig. 5). Then the conditions of destruction change. The crack at point O intersects the vertical line of symmetry. This indicates a change in the stress state, since on the vertical line of symmetry the parameters b_ξ and β_ξ in formulas (4)–(6) and (8) are equal to zero.

The shape of the truncated-wedge sample self-organizes into a wedge shape, and the parameters b_ξ and β_ξ act as the parameters of the so-called TMESS (Trajectory of

Maximum Effective Shear Stresses) return η, with the mentioned parameters denoted as bη and βη. Strictly speaking, the destruction process progresses from bottom to top. However, the slip lines ξ and η are interchangeable. Therefore, the subsequent description, this time not of the truncated-wedge shape but of the wedge shape, will proceed from top to bottom. This approach is more illustrative (Fig. 5b).

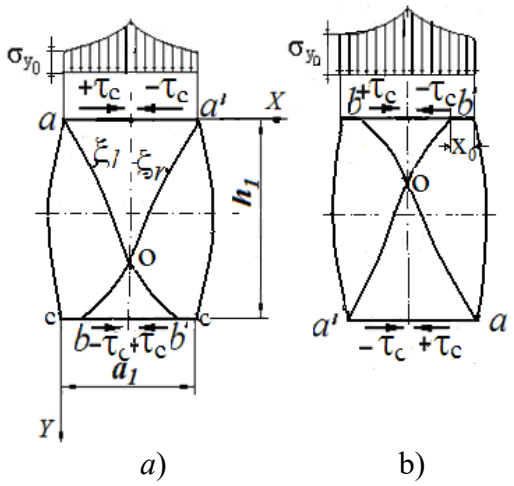

a) b)

Figure 5 – Scheme of destruction of a high specimen in the form of a wedge shape of destruction

At $h_1 = 1.5 \cdot a_1$ a wedge-shaped failure form arises, with the starting point of the failure on the contact surface located at a distance from the corner point equal to $x_0 = 0.15 \cdot a_1$ (Fig. 5). At $h_1 = 1.65 \cdot a_1$ the failure begins at one of the corner points of the sample. As the height of the sample increases, the starting point of the failure shifts to the lateral surface of the sample (Fig. 6). Thus, under the given physical and mechanical properties: $k_n = 10$ MPa, $\rho = 45°$, $f_c = 0.25$ and with a change in the sample height within $h_1 = (1.15–1.65) \cdot a_1$, the failure will occur in a wedge-shaped form, and the starting points of the failure will be located on the end surface at a distance from the right point a'.

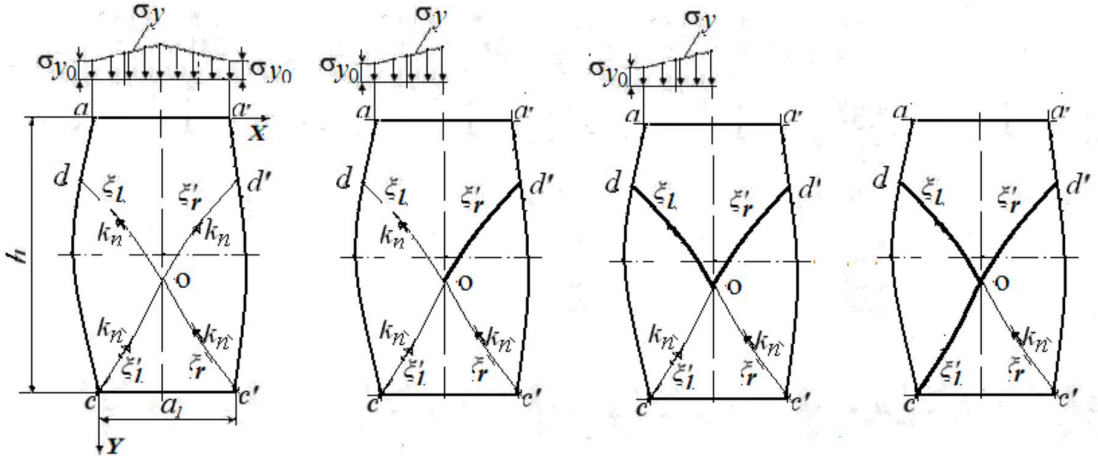

a) – at the time of pre-destruction; *b*) – at the time of the formation of the wedge side; *c*) – at the time of wedge formation; *d*) – at the time of wedge form formation

Figure 6 – Diagram of the formation of a wedge shape of a high prismatic rock sample for its compression at the beginning of fracture from the lateral surface

At a specimen height equal to $h_1 = 2 \cdot a_1$, with the parameters of the physical and mechanical properties of the material $k_n = 10$ MPa, $\mu = 1.0$, $f_c = 0.25$ The coordinates of the point of origin of destruction are: $x_0 = 0$; $y = 0.2$.

3. Conclusions

1. A mathematical model for the failure of high prismatic rock samples has been developed, utilizing four indicators (shear strength of the material, coefficients of internal and contact friction, and the modulus of elasticity) of rock properties, which allows for revealing the physical characteristics of the failure of high samples.

2. A prismatic sample with the material properties of the rock: $k_n = 10$ MPa, $\mu = 1.0$, $f_c = 0.25$, $E = 5.9 \cdot 10^4$ MPa before $h_1 = 1.15 \cdot a_1$ fails in the form of a truncated-wedge shape. As the sample height increases, the failure surface intersects the vertical symmetry line, and the failure occurs in a wedge-shaped form. When $h_1 = 1.65 \cdot a_1$ Failure begins at one of the corner points of the sample. As the height of the sample increases, the starting point of the failure shifts to the lateral surface of the sample.

REFERENCES

1. Geotechnical and Geological Engineering (2024), available at: https://link.springer.com/journal/10706 (Accessed 16 November 2024).

2. Comprehensive Mechanics of Materials (2024), Reference Work, First Edition, available at: https://www.sciencedirect.com/referencework/9780323906470/comprehensive-mechanics-of-materials (Accessed 16 November 2024).

3. Meille, S. (2024), "Methods of Determination of Young's Modulus and Tensile, Flexural and Compressive Strength", in Comprehensive Mechanics of Materials, Reference Work, First Edition, available at: https://www.researchgate.net/publication/341949754_Methods_of_Determination_of_Young's_Modulus_and_Tensile_Flexural_Compressive_Strength (Accessed 16 November 2024).

4. Vasilev, L.M., Vasilev, D.L., Malich, N.G. and Angelovskii, A.A. (2018), *Mekhanika obrazovaniya form razrusheniya obraztsov gornikh porod pri ikh szhatii* [The mechanics of the formation of failure patterns in rock samples under compression], IMA-press, Dnipro, Ukraine.

5. Li, M., Deng, H. and Tu, G. (2024), "A study of rock mass properties based on discrete fracture network modeling and compression damage process", *Bulletin of Engineering Geology and the Environment*, no. 83, p. 402. https://doi.org/10.1007/s10064-024-03898-1.

6. Bespalko, A., Dann, D., Petrov, M., Pomishin, E., Utsyn, G. and Fedotov, P. (2023), "Acoustic-Electrical Testing of Changes in the Stress–Strain State on the Example of Rock Samples", in Lysenko, E., Rogachev, A. and Starý, O. (eds.), *Recent Developments in the Field of Non-Destructive Testing, Safety and Materials Science*, ICMTNT 2021. Studies in Systems, Decision and Control, vol. 433, https://doi.org/10.1007/978-3-030-99060-2_22.

7. Chajed, S. and Singh, A. (2024), "Acoustic Emission (AE) Based Damage Quantification and Its Relation with AE-Based Micromechanical Coupled Damage Plasticity Model for Intact Rocks", *Rock Mechanics and Rock Engineering*, no. 57, pp. 2581–2604, https://doi.org/10.1007/s00603-023-03686-5.

8. Zhao, Y. and Borja, R.I. (2022), "A double-yield-surface plasticity theory for transversely isotropic rocks", *Acta Geotechnica*, no. 17, pp. 5201–5221, https://doi.org/10.1007/s11440-022-01605-6.

9. Yang, Y., Li, X. and Ju, Y. (2022), "Influence mechanisms of plasticity and horizontal stress difference on the fracture propagation in plastic reservoir rocks: a 3D XFEM-based plastic fracturing model", *Geomechanics and Geophysics for Geo-Energy and Geo-Resources*, no. 8, p. 145. https://doi.org/10.1007/s40948-022-00453-8.

10. Kovrizhnykh, A.M., Baryshnikov, V.D. and Khmelinin, A.P. (2023) 'Determining Time-to-Failure in Rocks Using Long-Term Strength Criterion', *Journal of Mining Science*, no. 59, pp. 911–918. https://doi.org/10.1134/S1062739123060042.

About the authors

Vasilyev Leonid, Doctor of Technical Sciences (D.Sc.), Professor, Senior Researcher in Department of Pressure Dynamics Control in Rocks, M.S. Poliakov Institute of Geotechnical Mechanics of the National Academy of Sciences of Ukraine (IGTM of the NAS of Ukraine), Dnipro, Ukraine, vleonid1937@gmail.com ORCID ***0000-0002-8146-0812***

Vasyliev Dmytro, Doctor of Technical Sciences (D.Sc.), Senior Researcher, Senior Researcher in Department of Elastomeric Component Mechanics in Mining Machines, M.S. Poliakov Institute of Geotechnical Mechanics of the National Academy of Sciences of Ukraine (IGTM of the NAS of Ukraine), Dnipro, Ukraine, vasyliev.d.l@dsau,dp.ua ORCID ***0000-0001-6864-357X***

Krasovskyi Ihor, Candidate of Technical Sciences (Ph.D)., Researcher, Department of Rock Mechanics, M.S. Poliakov Institute of Geotechnical Mechanics of the National Academy of Sciences of Ukraine (IGTM, NASU), Dnipro, Ukraine, ISKrasovsky@nas.gov.ua ORCID **0000-0002-4122-4292**

Rizo Zakhar, Ph.D. Student, Department of Elastomeric Component Mechanics in Mining Machines, M.S. Poliakov Institute of Geotechnical Mechanics of the National Academy of Sciences of Ukraine (IGTM of the NAS of Ukraine), Dnipro, Ukraine, zaharrizo777@gmail.com ORCID ***0000-0002-8271-7886***

Kress Denys, Ph.D. Student, Department of Elastomeric Component Mechanics in Mining Machines, M.S. Poliakov Institute of Geotechnical Mechanics of the National Academy of Sciences of Ukraine (IGTM of the NAS of Ukraine), Dnipro, Ukraine, Denni7777777@gmail.com ORCID ***0009-0001-9504-5695***

МАТЕМАТИЧНА МОДЕЛЬ РУЙНУВАННЯ ВИСОКИХ ПРИЗМАТИЧНИХ ЗРАЗКІВ ГІРСЬКИХ ПОРІД З ВИСОКИМ ЗНАЧЕННЯМ КУТА ВНУТРІШНЬОГО ТЕРТЯ

Васильєв Л., Васильєв Д., Красовський І., Різо З., Кресс Д.

Анотація. Механічні властивості гірських порід є одним із найважливіших факторів, що визначають їхню стійкість до руйнування, що особливо значущо в контексті гірничодобувної промисловості та проведення гірничих робіт. Традиційно такі випробування регламентувалися ДСТУ, які передбачали стискання зразків правильної геометрії, таких як куби, призми та циліндри. Основною метою цих стандартів є визначення межі міцності на стиск, що є ключовим показником для оцінки стійкості матеріалу під впливом навантажень. Випробування проводяться на зразках із висотою, незначно більшою за їхні поперечні розміри, що дозволяє найточніше змоделювати поведінку породи в умовах реальних гірських масивів.

Одним із головних параметрів для аналізу напружено-деформованого стану гірських порід є межа міцності та залишкова міцність, які оцінюються за діаграмами «напруження–деформація», отриманими під час руйнування зразків. Ці характеристики зазвичай визначаються на спеціалізованих пресах, доступних лише у великих наукових і дослідницьких центрах, таких як Інститут геотехнічної механіки НАН України та Криворізький національний технічний університет. Однак таке обладнання вимагає висококваліфікованого персоналу та регулярного обслуговування, а також розташоване на значній відстані від гірничодобувних підприємств. Це створює труднощі в отриманні оперативної інформації про міцність порід, що є особливо важливим для забезпечення безпеки гірничих робіт.

У цій статті запропоновано новий аналітичний метод розрахунку межі та залишкової міцності гірських порід, заснований на доступніших і простіших випробуваннях. Цей підхід дозволяє отримувати дані за чотирма основними параметрами: межа міцності на зсув, коефіцієнти внутрішнього та контактного тертя, а також модуль пружності матеріалу. Застосування такого методу не лише спрощує процес оцінки міцнісних характеристик, а й дозволяє точніше описати процеси руйнування високих зразків, що має практичне значення для інженерних розрахунків і проектування гірничих конструкцій. Відповідно до результатів досліджень, зі збільшенням висоти зразка його міцність помітно знижується: наприклад, при подвоєнні висоти гранична міцність може зменшитися на 30%.

Таким чином, запропонований аналітичний метод розширює можливості отримання даних про міцність гірських порід безпосередньо в польових умовах, що дозволяє оперативно оцінювати їхню стійкість і знижувати ризик аварійних ситуацій. Це сприяє підвищенню ефективності та безпеки гірничих робіт завдяки точнішому прогнозуванню поведінки гірських порід під навантаженням. Новий метод може бути корисним як для дослідницьких, так і для прикладних цілей, надаючи інженерам і проектувальникам інструмент для точнішого аналізу міцнісних характеристик порід.

Ключові слова: гірська порода; межа міцності; руйнування; тріщина; діаграма «напруження–деформація».